

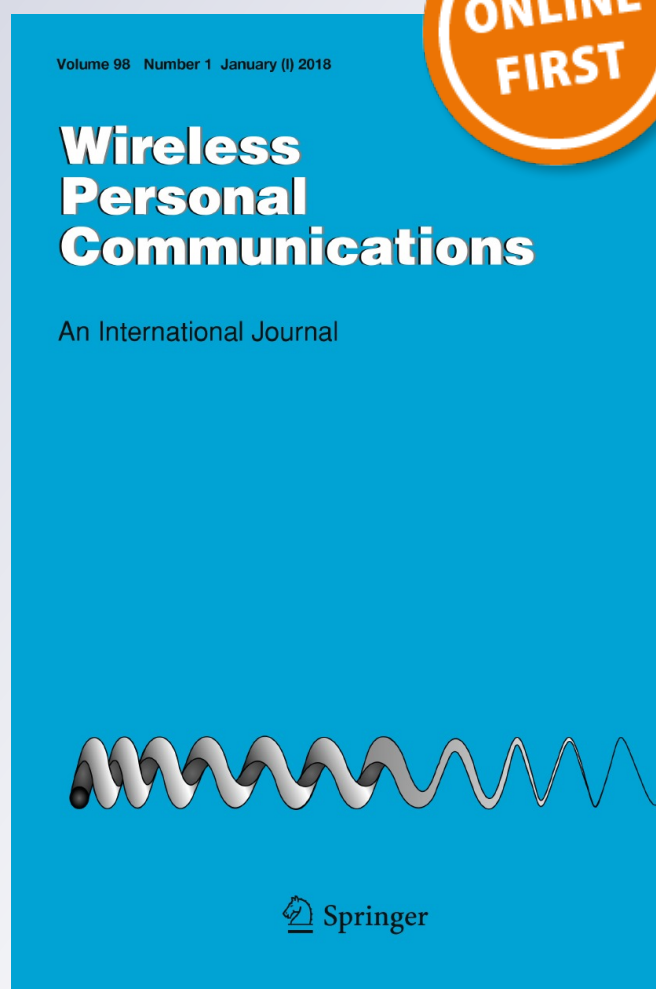
Iterative Joint Channel Estimation and Signal Detection for OFDM System in Double Selective Channels

Yih-Haw Jan

Wireless Personal Communications
An International Journal

ISSN 0929-6212

Wireless Pers Commun
DOI 10.1007/s11277-017-5184-1



Your article is protected by copyright and all rights are held exclusively by Springer Science+Business Media, LLC, part of Springer Nature. This e-offprint is for personal use only and shall not be self-archived in electronic repositories. If you wish to self-archive your article, please use the accepted manuscript version for posting on your own website. You may further deposit the accepted manuscript version in any repository, provided it is only made publicly available 12 months after official publication or later and provided acknowledgement is given to the original source of publication and a link is inserted to the published article on Springer's website. The link must be accompanied by the following text: "The final publication is available at link.springer.com".

Iterative Joint Channel Estimation and Signal Detection for OFDM System in Double Selective Channels

Yih-Haw Jan^{1,2,3} 

© Springer Science+Business Media, LLC, part of Springer Nature 2017

Abstract Intercarrier interference caused by fast time-varying multipath fading channels degrades the system performance of high-mobility orthogonal frequency division multiplexing systems. This study considers the challenging problem of joint channel estimation and signal detection in high mobility environments. The estimation method is based on a pilot-aided linear approximation channel modeling and iterative process. After each iteration, the channel estimates are refined with the fed-back detection signal. The channel is re-estimated iteratively, detected increasingly reliable signals. The proposed method is independent of the Doppler-spectrum, delay-profile shape and the number of paths. Numerical simulation results indicate that the proposed method is highly robust to fast time-varying multipath fading channels.

Keywords OFDM · Iterative method · Joint channel estimation and signal detection · Linear approximation channel model

1 Introduction

Orthogonal frequency-division multiplexing (OFDM) has become a key air interface for modern wireless communication systems such as Long Term Evolution Advanced (LTE-A), digital video broadcasting (DVB), and wireless local area networks. This is because OFDM has a high spectrum efficiency, simple implementation, robustness to frequency-

✉ Yih-Haw Jan
how@nkut.edu.tw

¹ Department of Digital Living Innovation, Nan Kai University of Technology, No. 568, Zhongzheng Rd., Caotun Township 54243, Nantou County, Taiwan, ROC

² Department of Mechanical Engineering, Nan Kai University of Technology, No. 568, Zhongzheng Rd., Caotun Township 54243, Nantou County, Taiwan, ROC

³ Department of Gerontic Technology and Service Management, Nan Kai University of Technology, No. 568, Zhongzheng Rd., Caotun Township 54243, Nantou County, Taiwan, ROC

selective channels and intersymbol interference (ISI) free transmission if the cyclic prefix (CP) is longer than the channel delay spread.

Coherent OFDM communication systems need accurate channel estimation for detecting the received signal in order to improve the OFDM system performance and the throughput of orthogonal frequency division multiple access (OFDMA) systems. The pilot-aided channel estimation is usually considered in the case of OFDM mobile communications [1]. The known training symbols are generally blended in the data payload to improve the channel estimation accuracy. Signal detection is then performed after the channel estimation is completed. In practice, the receiver can only obtain an imperfect estimate of the channel, regardless of the channel estimation method. Consequently, inaccurate channel estimation significantly degrade the detection performance.

Existing OFDM channel estimation methods are categorized into two major types, depending on whether the OFDM symbol duration exceeds the channel coherent time. The fading channel can be regarded as stationary when the duration within one OFDM symbol is much smaller than the channel coherent time. In this scenario, the fading in each subcarrier can be estimated and compensated independently [2].

Second, when the OFDM symbol duration is larger than the channel coherent time, the channel time variation causes inter-carrier interference (ICI). The ICI significantly affects system performances, and is particularly acute when the speed of motion increases [3]. In high speed motion scenarios, the fast time-varying channels during communication will be raised due to the Doppler spread. Therefore, channel estimation and signal detection become crucial issues in system design under such environments. In order to overcome the problems in fast time varying multipath fading channels, several methods have been presented to suppress the ICI.

Channel estimation of fast time-varying multipath fading channels for OFDM system can be performed in three methods, namely frequency domain [4, 5], time domain [6, 7], and hybrid [1, 8–11]. Frequency domain method is typically the simplest, since it treats the frequency domain channel matrix as either a diagonal or a banded matrix. Namely, the frequency-domain method disregards large ICI, and therefore suffers from an estimate error floor when the channels have large Doppler spreads. The time domain method performs poorly at determining the appropriate number of paths in a large channel delay spread. This task is very difficult because one OFDM symbol in a fast time-varying multipath channel has more number of unknown channel gains and time delays than received signals. An iterative LS method with ICI mitigation process [7] was presented for directly estimating the channel gains, but requires knowledge of the delay-related information.

The hybrid method models the time-varying channels by basis expansion (BEM). The advantage of this method is the low cost in realization since it only needs to estimate the basis coefficients. Hence, it can efficiently decrease the number of unknown channel model parameters below the number of unknown channel response parameters. Polynomial BEM (P-BEM) models using multi-symbol processes can provide accurate estimation for high a Doppler spread without ICI mitigation [1, 10, 11], but these require using the pure training symbols. However, the pilots and data are often mixed-jointly distributed on the pilot pattern in a typically system (e.g., for WiMAX and LTE). This approach is more complex in channel estimation but guarantees less throughput waste. Hence, a good channel estimator should not limit itself to using only training symbols. Additionally, some methods assume that variations of the channel impulse response during an OFDM symbol can be approximated with first-order polynomial. Some methods [8, 9] approximate the variation of each channel path using a piece-wise linear model based on the average gains of all

channel paths and the corresponding slopes in every OFDM symbol. The channel model is estimated from the CP or from both adjacent OFDM symbols. The iterative process is used in [8] to enhance the estimation of the slope using the detected signal. To lower the complexity of ICI mitigation, the estimate of the slope only processes the signals in CP. However, the residual ICI remains large and implementing the signal detection makes the algorithm highly complex [1].

This study considers the hybrid method in an iterative joint channel estimation and signal detection for OFDM systems in rapidly time-varying multipath fading channels, in order to achieve good performance operating over highly mobile wireless environments. The ICI on data subcarriers is estimated iteratively, then mitigated at each iterative step. The most reliable detected signals at data subcarriers are then purified as “virtual pilots”. The “virtual pilots” and the actual pilots can be combined as the “virtual training symbol”. Through the “virtual training symbol”, the channel estimation can filter out the interference and noise efficiently, and capture the channel variations well.

The remainder of this paper is organized as follows. Section 2 describes the baseband OFDM system model. Section 3 describes an iterative joint channel estimation and signal detection method based on linear approximation and discusses the complexity of the proposed method. Section 4 analyzes the characteristics of the proposed channel estimator. Section 5 presents some simulation results. Finally, Sect. 6 concludes the paper.

2 System Description

Consider a discrete-time model baseband equivalent OFDM system with N subcarriers, and a cyclic prefix (CP) length N_g . Let $\mathbf{X} = [X(0) X(1) \dots X(N-1)]^T$ indicate the input complex symbols for an OFDM symbol. By N -point inverse discrete Fourier transform (IDFT), the transmitted baseband signal is $\mathbf{x} = [x(0) x(1) \dots x(N-1)]^T$, where

$$x(k) = \frac{1}{\sqrt{N}} \sum_{n=0}^{N-1} X(n) e^{j\frac{2\pi}{N}kn} \tag{1}$$

where $k = -N_g, -N_g + 1, \dots, N - 1$.

Let $g_l(k)$ denote the time-variant channel gain of the path l at time instant k , where $l = 0, 1, \dots, L - 1$, and L represents the number of multipaths. At the receiver side, after removing CP, the received signal is

$$y(k) = \sum_{l=0}^{L-1} g_l(k)x(k-l) + z(k) \tag{2}$$

where $k = 0, 1, \dots, N - 1$, and $z(k)$ is the complex additive white Gaussian noise (AWGN) with zero-mean and variance σ_z^2 . The overall system can be expressed in matrix notation as:

$$\mathbf{y} = \mathbf{G}\mathbf{x} + \mathbf{z} \tag{3}$$

where $\mathbf{y} = [y(0) y(1) \dots y(N-1)]^T \in \mathbb{C}^{N \times 1}$ represents the received data vector after the CP removal; $\mathbf{z} = [z(0) z(1) \dots z(N-1)]^T \in \mathbb{C}^{N \times 1}$ denotes the Gaussian noise vector; $(\cdot)^T$ denotes the transpose operator, $\mathbf{G} \in \mathbb{C}^{N \times N}$ is the channel matrix in the time domain:

$$\mathbf{G} = \begin{bmatrix} g_0(0) & 0 & \cdots & 0 & g_{L-1}(0) & g_{L-2}(0) & \cdots & g_1(0) \\ g_1(1) & g_0(1) & 0 & \cdots & 0 & g_{L-1}(1) & \cdots & g_2(1) \\ \vdots & \ddots & \ddots & & & & & \vdots \\ 0 & \cdots & 0 & g_{L-1}(N-1) & g_{L-2}(N-1) & \cdots & \cdots & g_0(N-1) \end{bmatrix} \quad (4)$$

After DFT, the received signal in the frequency domain is

$$\mathbf{Y} = \mathbf{H}\mathbf{X} + \mathbf{Z} \quad (5)$$

where channel matrix $\mathbf{H} \in \mathbb{C}^{N \times N}$, $\mathbf{Y} = [Y(0) Y(1) \dots Y(N-1)]^T \in \mathbb{C}^{N \times 1}$, and $\mathbf{Z} = [Z(0) Z(1) \dots Z(N-1)]^T \in \mathbb{C}^{N \times 1}$ indicates AWGN in the frequency domain. Each entry in the \mathbf{H} is

$$\mathbf{H}(m, n) = \frac{1}{N} \sum_{k=0}^{N-1} \sum_{l=0}^{L-1} g_l(k) e^{\frac{-j2\pi(mk+(l-k)n)}{N}} \quad (6)$$

where $m = 0, 1, \dots, N-1$, and $n = 0, 1, \dots, N-1$. The off-diagonal term of \mathbf{H} , i.e., $m \neq n$, is the ICI response. If ICI mitigation is perfectly performed, then the ICI response is cancelled and the diagonal term represents the channel frequency response (CFR).

3 Channel Estimation Based on Linear Approximation Channel Model

The channel variation of each multipath is often modeled to be linear in an OFDM symbol duration $N_s = N_g + N$. The linear approximation channel can be written as

$$g_l(k) = c_{0,l} + c_{1,l}k \quad (7)$$

where $k = -N_g, -N_g + 1, \dots, N-1$; $c_{0,l}$ and $c_{1,l}$ are the average and slope of channel path l .

Substitute (7) into (6), then the channel matrix is

$$\mathbf{H} = \mathbf{H}_0 + \mathbf{H}_1 \quad (8)$$

where each entry in \mathbf{H}_0 and \mathbf{H}_1 is

$$\begin{aligned} \mathbf{H}_0(m, n) &= \frac{1}{N} \sum_{k=0}^{N-1} \sum_{l=0}^{L-1} c_{0,l} e^{\frac{-j2\pi(mk+(l-k)n)}{N}} \\ &= \sum_{l=0}^{L-1} c_{0,l} \frac{1}{N} \sum_{k=0}^{N-1} e^{\frac{-j2\pi(mk+(l-k)n)}{N}} \\ &= \varphi_0^{(m,n)} \mathbf{C}_0 \end{aligned} \quad (9)$$

and

$$\begin{aligned}
 \mathbf{H}_1(m, n) &= \frac{1}{N} \sum_{k=0}^{N-1} \sum_{l=0}^{L-1} c_{1,l} e^{-\frac{j2\pi(mk+(l-k)n)}{N}} \\
 &= \sum_{l=0}^{L-1} c_{1,l} \frac{1}{N} \sum_{k=0}^{N-1} k e^{-\frac{j2\pi(mk+(l-k)n)}{N}} \\
 &= \boldsymbol{\varphi}_1^{(m,n)} \mathbf{C}_1
 \end{aligned} \tag{10}$$

for $m = 0, 1, \dots, N - 1$; $n = 0, 1, \dots, N - 1$; $\mathbf{C}_0 = [c_{0,0} \ c_{0,1} \ \dots \ c_{0,L-1}]^T \in \mathbb{C}^{L \times 1}$, $\mathbf{C}_1 = [c_{1,0} \ c_{1,1} \ \dots \ c_{1,L-1}]^T \in \mathbb{C}^{L \times 1}$; $\boldsymbol{\varphi}_0^{(m,n)} \in \mathbb{C}^{1 \times L}$ and $\boldsymbol{\varphi}_1^{(m,n)} \in \mathbb{C}^{1 \times L}$ with

$$\boldsymbol{\varphi}_0^{(m,n)}(l) = \frac{1}{N} \sum_{k=0}^{N-1} e^{-\frac{j2\pi(mk+(l-k)n)}{N}} \tag{11}$$

and

$$\boldsymbol{\varphi}_1^{(m,n)}(l) = \frac{1}{N} \sum_{k=0}^{N-1} k e^{-\frac{j2\pi(mk+(l-k)n)}{N}} \tag{12}$$

where $l = 0, 1, \dots, L - 1$.

Now consider equi-spaced N_p pilots for the time variant channel estimation. Assume that N/N_p is an integer, the N_p pilot subcarriers are at index set $\mathcal{S}_p = \{p_i = i \times (N/N_p) \mid i = 0, 1, \dots, N_p - 1\}$. The rest of $N - N_p$ data subcarriers are at index set \mathcal{S}_d . For convenience, let

$$\mathbf{X}_p = \mathbf{Z}pad(\mathbf{X}, \mathcal{S}_d) \tag{13}$$

and

$$\mathbf{X}_d = \mathbf{Z}pad(\mathbf{X}, \mathcal{S}_p) \tag{14}$$

where \mathbf{X}_p and \mathbf{X}_d are padding \mathbf{X} with zeros in the rows belonging to \mathcal{S}_d and \mathcal{S}_p , respectively. Hence we have $\mathbf{X} = \mathbf{X}_p + \mathbf{X}_d$.

$$\mathbf{X} = \mathbf{X}_p + \mathbf{X}_d \tag{15}$$

Substitute (8) and (15) into (5) to

$$\begin{aligned}
 \mathbf{Y} &= \mathbf{H}\mathbf{X} + \mathbf{Z} \\
 &= \mathbf{H}(\mathbf{X}_p + \mathbf{X}_d) + \mathbf{Z} \\
 &= (\mathbf{H}_0 + \mathbf{H}_1)\mathbf{X}_p + \mathbf{H}\mathbf{X}_d + \mathbf{Z}
 \end{aligned} \tag{16}$$

Since \mathbf{X}_d is unknown data, the term $\mathbf{H}\mathbf{X}_d$ in (16) is the interference induced by data subcarriers. The expression becomes

$$\mathbf{Y} = \mathbf{U}_0\mathbf{C}_0 + \mathbf{U}_1\mathbf{C}_1 + \mathbf{J} + \mathbf{Z} \tag{17}$$

where $\mathbf{J} = \mathbf{H}\mathbf{X}_d \in \mathbb{C}^{N \times 1}$; and each entry in \mathbf{U}_0 and \mathbf{U}_1 is

$$\begin{aligned} \mathbf{U}_0(m, l) &= \frac{1}{N} \sum_{n=0}^{N-1} \mathbf{X}_p(n) \sum_{k=0}^{N-1} e^{\frac{-j2\pi(mk+(l-k)n)}{N}} \\ &= \boldsymbol{\psi}_0^{(m,l)} \mathbf{X}_p \end{aligned} \tag{18}$$

and

$$\begin{aligned} \mathbf{U}_1(m, l) &= \frac{1}{N} \sum_{n=0}^{N-1} \mathbf{X}_p(n) \sum_{k=0}^{N-1} (k - N_c) e^{\frac{-j2\pi(mk+(l-k)n)}{N}} \\ &= \boldsymbol{\psi}_1^{(m,l)} \mathbf{X}_p \end{aligned} \tag{19}$$

for $m = 0, 1, \dots, N - 1$; $l = 0, 1, \dots, L - 1$; $\mathbf{U}_0 \in \mathbb{C}^{N \times L}$; $\mathbf{U}_1 \in \mathbb{C}^{N \times L}$; $\mathbf{U}_0 \mathbf{C}_0 = \mathbf{H}_0 \mathbf{X}_p$; $\mathbf{U}_1 \mathbf{C}_1 = \mathbf{H}_1 \mathbf{X}_p$; and each entry in $\boldsymbol{\psi}_0^{(m,l)} \in \mathbb{C}^{1 \times N}$ and $\boldsymbol{\psi}_1^{(m,l)} \in \mathbb{C}^{1 \times N}$ is

$$\boldsymbol{\psi}_0^{(m,l)}(n) = \frac{1}{N} \sum_{k=0}^{N-1} e^{\frac{-j2\pi(mk+(l-k)n)}{N}} \tag{20}$$

and

$$\boldsymbol{\psi}_1^{(m,l)}(n) = \frac{1}{N} \sum_{k=0}^{N-1} k e^{\frac{-j2\pi(mk+(l-k)n)}{N}} \tag{21}$$

where $n = 0, 1, \dots, N - 1$.

Each entry of $\boldsymbol{\psi}_0^{(m,l)}$ and $\boldsymbol{\psi}_1^{(m,l)}$ can be pre-computed and stored at the receiver, since it does not depend on the unknown data.

3.1 Channel Estimation Using Pilot Subcarriers

For an algebra solution, let $\mathbf{U} = [\mathbf{U}_0 \ \mathbf{U}_1] \in \mathbb{C}^{N \times 2L}$ and $\mathbf{C} = [\mathbf{C}_0^T \ \mathbf{C}_1^T]^T = [c_{0,0} \ c_{0,1} \ \dots \ c_{0,L-1} \ c_{1,0} \ c_{1,1} \ \dots \ c_{1,L-1}]^T \in \mathbb{C}^{2L \times 1}$, then (17) becomes

$$\begin{aligned} \mathbf{Y} &= \mathbf{UC} + \mathbf{J} + \mathbf{Z} \\ &= \mathbf{UC} + \mathbf{E} \end{aligned} \tag{22}$$

where $\mathbf{E} = \mathbf{J} + \mathbf{Z}$.

Let $\mathbf{Y}^{(p)}$ and $\mathbf{E}^{(p)}$ indicate vectors of size N_p with the sampled elements of \mathbf{Y} and \mathbf{E} belonging to \mathcal{S}_p , respectively. Additionally, let $\mathbf{U}^{(p)}$ represent the submatrix of size $N_p \times 2L$ formed with the rows of \mathbf{U} belonging to \mathcal{S}_p . Thus, by sampling (22), the received signal at pilot positions is

$$\mathbf{Y}^{(p)} = \mathbf{U}^{(p)} \mathbf{C} + \mathbf{E}^{(p)} \tag{23}$$

Note that $\mathbf{E}^{(p)}$ comprises of a sum of many zero-mean uncorrelated random variables including interference induced from data subcarriers and additive noise. Hence, by the central limit theorem, each element in $\mathbf{E}^{(p)}$ can be assumed to be many zero-mean Gaussian variables. The least square (LS) solution of (23) is given by

$$\hat{\mathbf{C}} = \mathbf{U}^{(p)+} \mathbf{Y}^{(p)} \tag{24}$$

where $^+$ denotes the pseudo-inverse operation and $\hat{\mathbf{C}} = [\hat{c}_{0,0} \ \hat{c}_{0,1} \ \dots \ \hat{c}_{0,L-1} \ \hat{c}_{1,0} \ \hat{c}_{1,1} \ \dots \ \hat{c}_{1,L-1}]^T \in \mathbb{C}^{2L \times 1}$. Substitute (24) into (7), the estimated channel can be obtained. Since \mathbf{X}_p is already-known at the

receiver, the terms of $\mathbf{U}^{(p)}$, $\mathbf{U}_p^{(p)}$, and $\mathbf{U}_p^{(p)+}$ can be pre-computed and stored at the receiver. Note that the proposed method is independent from Doppler-spectrum, delay-profile shape, and the number of paths. The estimated $\hat{\mathbf{H}}$ is determined as

$$\begin{aligned} \hat{\mathbf{H}}(m, n) &= \hat{\mathbf{H}}_0(m, n) + \hat{\mathbf{H}}_1(m, n) \\ &= \boldsymbol{\varphi}_0^{(m,n)} \hat{\mathbf{C}}_0 + \boldsymbol{\varphi}_1^{(m,n)} \hat{\mathbf{C}}_1 \end{aligned} \tag{25}$$

Hence the signal detection at the pilot subcarriers can be obtained by

$$\hat{\mathbf{X}}_{p,0} = \text{Zpad}(Q[\hat{\mathbf{H}}^+ \mathbf{Y}], \mathbf{S}_d) \tag{26}$$

where function $Q[\cdot]$ represents the decision operation. The output of $Q[\cdot]$ is thus a quadrature amplitude modulation (QAM) constellation point.

The accuracy of the initial channel estimation decisively affects the performance at the later iterative process.

3.2 Iterative Method

The channel estimation is performed from the pilot information. However, the interference and noise impacts initial estimation accuracy. To resolve this drawback, the pilots are passed through the estimated channel approximating of the induced interference. Mathematically, this procedure can be expressed as

$$\begin{aligned} \mathbf{Y} &= \mathbf{H}\mathbf{X} + \mathbf{Z} \\ &= \mathbf{H}(\mathbf{X}_p + \mathbf{X}_d) + \mathbf{Z} \\ &= \mathbf{I}_p + \mathbf{H}\mathbf{X}_d + \mathbf{Z} \end{aligned} \tag{27}$$

where $\mathbf{I}_p = \mathbf{H}\mathbf{X}_p$ indicates the pilot induced interference. The value \mathbf{I}_p is subtracted from the received symbol

$$\mathbf{Y} - \mathbf{I}_p = \mathbf{H}\mathbf{X}_d + \mathbf{Z} \tag{28}$$

Now the pilot induced interference is reduced, improving the signal detection

$$\tilde{\mathbf{X}} = Q[\mathbf{H}^+(\mathbf{Y} - \mathbf{I}_p)] \tag{29}$$

The detected signals at the data subcarriers are

$$\tilde{\mathbf{X}}_d = \text{Zpad}(\tilde{\mathbf{X}}, \mathbf{S}_p) \tag{30}$$

Now we have the detected data. Let the detected signal be given by:

$$\bar{\mathbf{X}} = \mathbf{X}_p + \tilde{\mathbf{X}}_d \tag{31}$$

Next, channel estimation is performed through both the pilot and the detected data. Let $\hat{\mathbf{U}} = [\hat{\mathbf{U}}_0 \ \hat{\mathbf{U}}_1]$, where the elements in $\hat{\mathbf{U}}_0$ and $\hat{\mathbf{U}}_1$ are

$$\begin{aligned} \hat{\mathbf{U}}_0(m, l) &= \frac{1}{N} \sum_{n=0}^{N-1} \bar{\mathbf{X}}(n) \sum_{k=0}^{N-1} e^{\frac{-j2\pi(mk+(l-k)n)}{N}} \\ &= \boldsymbol{\psi}_0^{(m,l)} \bar{\mathbf{X}} \end{aligned} \tag{32}$$

and

$$\begin{aligned} \hat{U}_1(m, l) &= \frac{1}{N} \sum_{n=0}^{N-1} \bar{X}(n) \sum_{k=0}^{N-1} k e^{\frac{-j2\pi(mk+(l-k)n)}{N}} \\ &= \psi_1^{(m,l)} \bar{X} \end{aligned} \tag{33}$$

The new estimate, is thus:

$$\hat{C} = \hat{U} + Y \tag{34}$$

The refined estimation of H and g_l can thus be obtained. The refined signals can be detected

$$\hat{X} = Q[\hat{H} + Y] \tag{35}$$

The refined detection signal in the pilot subcarriers is

$$\hat{X}_p = Zpad(\hat{X}, S_d) \tag{36}$$

The next question is how to determine when to stop the iteration. This study presents an iteration stop criteria by checking the validity of the detected pilots in (35). Considering the iteration index l , the ‘‘pilot accuracy vector’’ $e^{(l)}$ is defined as follows:

$$e^{(l)}(k) = \begin{cases} 0, & \text{if } \hat{X}_p^{(l)}(k) = X_p(k) \\ 1, & \text{otherwise} \end{cases} \tag{37}$$

where $k \in S_p$. The proposed method is designed for iterative refinement of the channel estimation and data detection results. Hence, if $e^{(i-1)}(k) = 0$ from the last iteration but it becomes 1 on the current iteration (i.e., $e^{(i)}(k) = 1$), then the iteration process is stopped because the new process is not improved over the old one. Suppose at iteration i , the whole processing is summarized as follows

Step 1 Initialization of the channel estimation and signal detection from (25) and (26), setting the iteration index $i = 0$ for the estimated $H^{(i)}$ and $C^{(i)}$.

Step 2 At the iteration i , where $i = 1, 2, \dots, ITER$ (where $ITER$ represents the maximum number of iterations; if $i > ITER$, then end the iteration), calculate the pilot induced interference $\hat{I}_p^{(i)} = \hat{H}^{(i-1)} X_p$ and refine the received symbol $Y^{(i)} = Y - \hat{I}_p^{(i)}$.

Step 3 Perform signal detection using $Y^{(i)}$

$$\tilde{X} = Q[\hat{H}^{(i-1)} + Y^{(i)}] \tag{38}$$

Then the detected signals at the data subcarriers are

$$\tilde{X}_d = Zpad(\tilde{X}, S_p) \tag{39}$$

Let

$$\bar{X} = X_p + \tilde{X}_d \tag{40}$$

Step 4 Determine $U^{(i)}$ from the detected signal in (41), then we get

$$\hat{C}^{(i)} = U^{(i)} + Y \tag{41}$$

Step 5 Forming $\hat{H}^{(i)}$, which allows for better signal detection

$$\hat{\mathbf{X}}^{(i)} = \mathbf{Q}[\hat{\mathbf{H}}^{(i+)}\mathbf{Y}] \tag{42}$$

The refined detection signals in the pilot subcarriers and data subcarriers can be extracted by

$$\mathbf{X}_p^{(i)} = \mathbf{Z}_{pad}(\hat{\mathbf{X}}^{(i)}, \mathbf{S}_d) \tag{43}$$

Step 6 Check $\mathbf{e}^{(i)}(k)$ and $\mathbf{e}^{(i-1)}(k)$. If $\mathbf{e}^{(i-1)}(k) = 0$ and $\mathbf{e}^{(i)}(k) = 1$, then set the final refined channel estimation and data detection results as

$$\hat{\mathbf{C}} = \hat{\mathbf{C}}^{(i-1)} \tag{44}$$

and then end the iteration. Otherwise, increment the iteration number $i = i + 1$ and return to Step 2.

The pilot-induced interference is thus lowered, improving channel estimation and system performance.

To confirm verify that the iterative process is able to refine the estimate in the fast time-varying multipath fading channel, the COST 207 bad urban (BU) area channels (the number of resolvable paths of the channel is given by $L = 51$) at $f_dT = 0.1$ was employed to examine the estimation results. For example, an OFDM system with 5 MHz bandwidth at 2.5 GHz carrier frequency, $N = 512$ subcarriers, CP length $N_g = N/8 = 64$, and there are $N_p = N/2 = 256$ pilot subcarriers in an OFDM symbol. The system used QPSK modulation with coherent demodulation. The vehicular speeds was about 400 km/h at $f_dT = 0.1$.

Consider $E_b/N_0 = 40$ dB, where E_b indicates the energy per bit and N_0 is the variance of the AWGN. Figure 1 illustrates a snapshot of the path variation of the true channel, initial estimate, and multiple iterative processes. The figure shows that the initial estimates on both the real and imaginary parts are away from the true channels. An improved approximation to the real and imaginary part of the original $g_A(k)$ can be achieved with three iteration estimates. The closest estimate is achieved after the third iteration. The approximations to the true channels improve slightly from the second to the third iteration.

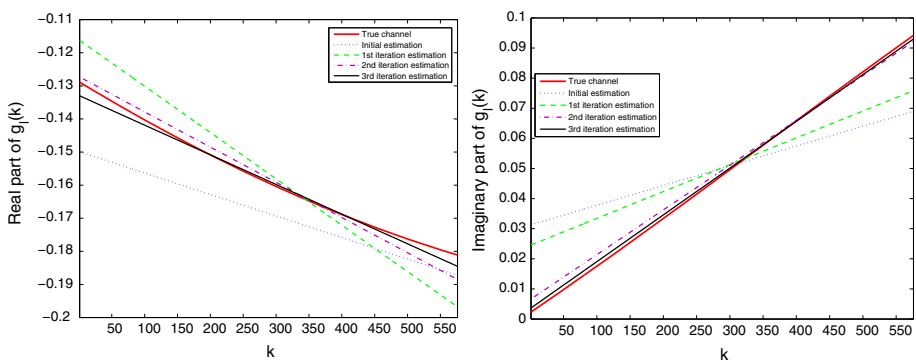


Fig. 1 Comparisons of snapshot of path variation between true and estimated $g_A(k)$ for $E_b/N_0 = 40$ dB using the proposed method under COST 207 BU channels at $f_dT = 0.1$. A channel variation of a path across one OFDM symbol. Left: Real part; right: Imaginary part

3.3 Computational Complexity Analysis

This subsection shows the verification of the key computational complexities above, based on the required complex multiplications (CMULTs).

The key computations of the initialization step are the estimation of \hat{C} in (21), channel matrix reconstruction in (22) and signal detection in (23). Because X_p is known at the receiver, $U^{(p)+}$ can be pre-computed and stored at the receiver. Hence (21) requires $2N_p L$ CMULTs. In (22), each \hat{H} performs $4N^2L$ CMULTs. From (23), \hat{H}^+ and \hat{H}^+Y require $5N^3$ and N^2 CMULTs, respectively [12]. Table 1 summarizes the computational complexity in the initialization step.

The main complexity in the iteration procedure in Steps 2–4. In step 2, the pilot-induced interference $\hat{I}_p^{(i)} = \hat{H}^{(i-1)}X_p$ can be determined with N^2 CMULTs. The signal detection in Step 3 for calculating \hat{H}^+ and $\hat{H}^+Y^{(i)}$ requires $5N^3$ and N^2 CMULTs, respectively. In Step 4, computing $\hat{U}^{(i)}$ needs $2N^2L$ CMULTs; calculating $\hat{U}^{(i)+}$ requires $6N^2L + 8NL^2$ CMULTs; $\hat{U}^{(i)+}Y^{(i)}$ is obtained using $2NL$ CMULTs. In Step 5, updating $\hat{H}^{(i)}$ requires $4N^2L$ CMULTs, while updating $\hat{H}^{(i)+}$ and $\hat{H}^{(i)+}Y^{(i)}$ needs $5N^3$ and N^2 CMULTs, respectively. No product computation is performed in Step 6. Table 2 summarizes the computational complexity after each iteration in the iteration process.

For example, consider a system with IDFT size $N = 512$. Let the CP length $N_g = N/8 = 64$ and the number of pilot subcarriers $N_p = N/2 = 256$. For convenience, assume that N_g equals the number of channel paths, i.e., $L = N_g = 64$. The rightmost column in Table 1 lists the required number of CMULTs of the initialization step in this example.

Table 2 presents the ratio of computational complexity between the proposed method and the traditional method [8]. The traditional method [8], based on interference mitigation, iteratively estimates the channel gain and slope within an OFDM symbol. The complexity analysis of [8] is presented in [1]. As seen in Table 3, the computational complexity ratios between the proposed and traditional methods are 101.0, 104.2, and 105.7% for first, second and third iterations, respectively. These ratios are very close to 1. Namely, the computational complexities of the proposed and traditional methods are similar. However, the proposed method has far superior performance to the traditional method.

4 Performance Analysis

This section presents the performance analysis of the proposed iterative method in a noisy channel. For convenience, the following analysis disregards the iteration index.

Table 1 Computational complexity of initialization step

| Computing | No. of CMULTs | No. of CMULTs for $N = 512$, $N_p = 256$, and $L = 64$ |
|-------------------------------|------------------------------|--|
| $\hat{C} = U_p^{(p)+}Y^{(p)}$ | $2N_pL$ | 32,768 |
| Forming \hat{H} | $4N^2L$ | 67,108,864 |
| \hat{H}^+ | $5N^3$ | 671,088,640 |
| \hat{H}^+Y | N^2 | 262,144 |
| Total | $2N_pL + 4N^2L + 5N^3 + N^2$ | 738,492,416 |

Table 2 Computational complexity for the iteration process

| Step | Computing | No. of CMULTs | No. of CMULTs for $N = 512$, $N_p = 256$, and $L = 64$ |
|-------|---|-----------------|---|
| 2 | $\hat{\mathbf{f}}_p^{(i)} = \hat{\mathbf{H}}^{(i-1)}\mathbf{X}_p$ | N^2 | 262,144 |
| 3 | $\hat{\mathbf{H}}^+ \mathbf{Y}^{(i)}$ | N^2 | 262,144 |
| 4 | Forming $\hat{\mathbf{U}}^{(i)}$ | $2N^2L$ | 33,554,432 |
| | $\hat{\mathbf{U}}^{(i)+}$ | $6N^2L + 8NL^2$ | 117,440,512 |
| | $\hat{\mathbf{U}}^{(i)+} \mathbf{Y}^{(i)}$ | $2NL$ | 65,536 |
| 5 | Forming $\hat{\mathbf{H}}^{(i)}$ | $4N^2L$ | 67,108,864 |
| | $\hat{\mathbf{H}}^{(i)+}$ | $5 N^3$ | 671,088,640 |
| | $\hat{\mathbf{H}}^{(i)+} \mathbf{Y}$ | N^2 | 262,144 |
| 6 | – | – | 0 |
| Total | $5N^3 + 12N^2L + 3N^2 + 8NL^2 + 2NL$ | | 890,044,416 |

Table 3 Ratio of computational complexity between the proposed and traditional methods [8]

| Estimation method | The conventional method ITER iterations | | |
|---------------------|---|-------|-------|
| | 1 | 2 | 3 |
| Proposed method (%) | 101.0 | 104.2 | 105.7 |

To start, express the l th exact linear channel model \mathbf{g}_l in a vector–matrix form:

$$\mathbf{g}_l = \mathbf{V}_l \mathbf{C} \tag{45}$$

where $\mathbf{g}_l = [\mathbf{g}_l(0) \mathbf{g}_l(1) \dots \mathbf{g}_l(N - 1)]^T$ for $l = 0, 1, \dots, L - 1$, and \mathbf{V}_l is an $N \times 2L$ matrix:

$$\mathbf{V}_l(n, m) = \begin{cases} 1, & \text{if } m = l \\ 1, & \text{if } n = 0 \text{ and } m = L + l \\ n, & \text{if } n \neq 0 \text{ and } m = L + l \\ 0, & \text{otherwise} \end{cases} \tag{46}$$

for $n = 0, 1, \dots, N - 1$, and $m = 0, 1, \dots, 2L - 1$. The l th estimated \mathbf{g}_l is then written as

$$\hat{\mathbf{g}}_l = \mathbf{V}_l \hat{\mathbf{C}} \tag{47}$$

The error between the l th exact linear channel model and the l th estimated channel is given by

$$\begin{aligned} \mathbf{e}_l &= \hat{\mathbf{g}}_l - \mathbf{g}_l \\ &= \mathbf{V}_l(\hat{\mathbf{C}} - \mathbf{C}) \end{aligned} \tag{48}$$

Substituting (22) and (41) into (48) obtains:

$$\begin{aligned} \mathbf{e}_l &= -\mathbf{V}_l \mathbf{U}^+ (\mathbf{J} + \mathbf{Z}) \\ &= -\mathbf{B}_l (\mathbf{J} + \mathbf{Z}) \end{aligned} \tag{49}$$

where $\mathbf{B}_l = \mathbf{V}_l \mathbf{U}^+$.

The normalized mean-square error (NMSE) between the l th exact linear channel model and the l th estimated channel can be expressed as

$$NMSE_l = \frac{1}{N} \text{tr}\{E[\mathbf{e}_l \mathbf{e}_l^H]\} \tag{50}$$

where $E[\cdot]$ and $\text{tr}(\mathbf{A})$ represent the expectation and trace of matrix \mathbf{A} , respectively. Thus (49) and (50) yield:

$$NMSE_l = \frac{1}{N} \text{tr}\{E[\mathbf{B}_l (\mathbf{J} + \mathbf{Z})(\mathbf{J} + \mathbf{Z})^H \mathbf{B}_l^H]\} \tag{51}$$

Note that the covariance matrix of the interference and noise can be determined as

$$E[(\mathbf{J} + \mathbf{Z})(\mathbf{J} + \mathbf{Z})^H] = \mathbf{R}_J + \mathbf{R}_Z \tag{52}$$

where $\mathbf{R}_J = E[\mathbf{J}\mathbf{J}^H]$ and $\mathbf{R}_Z = E[\mathbf{Z}\mathbf{Z}^H]$.

Substituting (52) in (51) yields

$$\begin{aligned} NMSE_l &= \frac{1}{N} \text{tr}\{\mathbf{B}_l \mathbf{R}_J \mathbf{B}_l^H\} + \frac{\sigma_Z^2}{N} \text{tr}\{\mathbf{B}_l \mathbf{B}_l^H\} \\ &= \frac{1}{N} \text{tr}\{\mathbf{B}_l \mathbf{R}_J \mathbf{B}_l^H\} + \frac{\sigma_Z^2}{N} \sum_{n=0}^{N-1} \sum_{k=0}^{N-1} \|\mathbf{B}_l(n, k)\|^2 \end{aligned} \tag{53}$$

Clearly, the performance of the proposed method depends on the interference induced by data subcarriers (presented as \mathbf{R}_J). The proposed iterative method reduces interference term. The overall channel estimation NMSE is given by:

$$NMSE_l = \frac{\sigma_Z^2}{N} \sum_{n=0}^{N-1} \sum_{k=0}^{N-1} \|\mathbf{B}_l(n, k)\|^2 \tag{54}$$

5 Performance of the Presented Method

This section describes the performance of the proposed channel estimation method under a COST207 BU time-varying fading channel. An OFDM signal was generated from 5 MHz of channel bandwidth, divided into 512 subcarriers. The varying normalized Doppler frequencies were set at 0.025, 0.05, 0.075, and 0.1 implying vehicular speeds about 100, 200, 300, and 400 km/h, respectively, based on a carrier frequency is 2.5 GHz. According to the COST207 channel model, the number of resolvable paths of the channel is given by $L = 51$. The analysis was run using QPSK modulation with coherent demodulation. The pilot symbols were generated with PN sequences. The normalized mean-square error (NMSE) performances for each E_b/N_0 value were obtained from 7000 simulation runs.

The NMSE performances for each E_b/N_0 were compared between the proposed method and the traditional method [8], which also utilizes the linear approximation channel model to estimate the channel response within the duration of a single symbol. Figure 2 depicts

the middle-speed ($f_dT = 0.025$) and high-speed ($f_dT = 0.05$) car-mobility. Figure 3 considers the high-speed railway environments ($f_dT = 0.075$ and 0.1). The resulting curves correspond to performance without interference mitigation (the initial estimation), and at different iterations.

Figures 2 and 3 reveal that the traditional method yields a much worse performance than the initial estimation of the proposed method. The proposed method had an initial estimate of NMSE almost one order of magnitude better than the traditional method. Significant differences of the NMSE were observed between the initial estimation and iterative processes regardless of E_b/N_0 . The NMSE induced by the interference was improved by almost two orders of magnitude after three iterations. That is, the iterative process yielded an apparently improved performance. The performances of the proposed method are almost indistinguishable after the second iteration for $f_dT = 0.25$, because the linear interpolation can obtain a highly accurate estimation for smaller f_dT . For $f_dT = 0.05, 0.075$, and 0.1 , the difference in performances was very small after the third iteration. Simulation results reveal that three iterations can provide a sufficiently accurate estimation. The analytical results form an important foundation in making the method practical by limiting its computational complexity.

The bit-error-rate (BER) performance of the entire system depends on the channel estimation accuracy and the interference mitigation. Figures 4 and 5 illustrate BER performance comparisons with the BER of the zero-forcing (ZF) method in perfectly-known channels included for reference (see curves marked by “ZF in perfectly-known channel”). For fair comparison, the BER of the traditional method is also presented. The graphs demonstrate that BER of the initial estimation was degraded with rising ICI in proportion to f_dTs . In either channel, the relative performance of the initial estimation significantly outperformed the traditional method regardless of f_dTs and E_b/N_0 . The first iteration of our method lowered the BER by almost one order of magnitude from the initial estimate. The error floor of the conventional method was observed at $BER \approx 2 \times 10^{-1}$ for $f_dT = 0.1$ and $E_b/N_0 = 40$ dB. In contrast, the error floor of our initial estimation was founded at $BER = 2.5 \times 10^{-2}$. The BER was reduced to 3×10^{-3} after the first iteration was performed. Clearly, the BER that improved significantly between the initial estimation and iterative processes, irrespective of E_b/N_0 . Three iterations improved the BER induced by the ICI by more than one order of magnitude. The simulation results confirm that the iterative process yielded an apparent performance improvement. The performances were

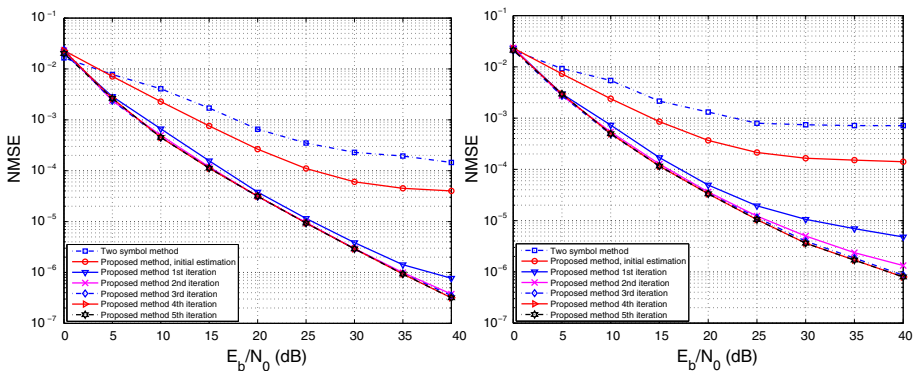


Fig. 2 NMSE comparison of the proposed method and traditional method [8] under the COST 207 BU channels. Left: $f_dT = 0.025$; right: $f_dT = 0.05$

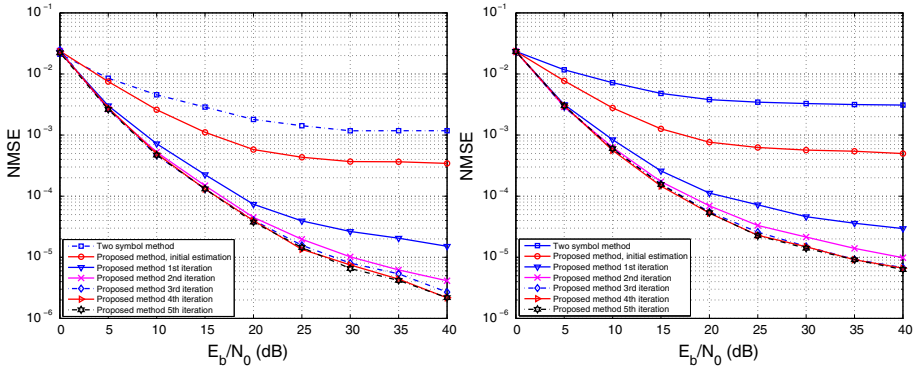


Fig. 3 NMSE performance of the proposed and traditional methods [8] under the COST 207 BU channels. Left: $f_d T = 0.075$; right: $f_d T = 0.1$

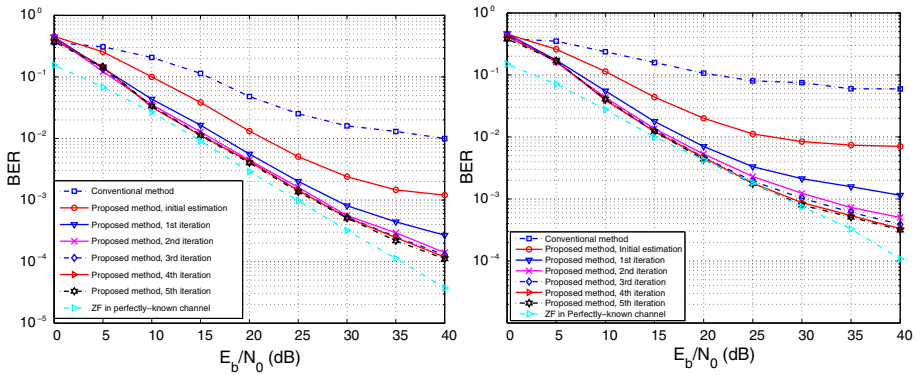


Fig. 4 BER performances of different methods under the COST 207 BU channels. Left: $f_d T = 0.025$; right: $f_d T = 0.05$

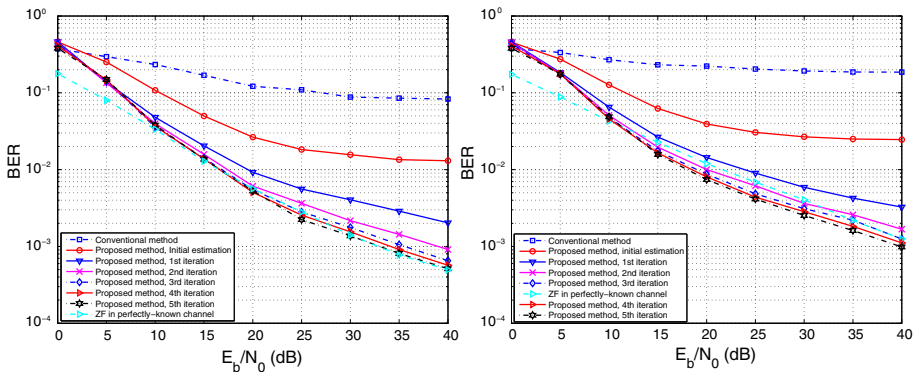


Fig. 5 BER performances of different methods under the COST 207 BU channels. Left: $f_d T = 0.075$; right: $f_d T = 0.1$

almost indistinguishable after the second iteration for $f_d T = 0.025$. The performance difference in BER three iterations was found to be very small for $f_d T = 0.05, 0.075, \text{ and } 0.1$.

Moreover, as seen in Figs. 4 and 5, BER performances of the proposed method were comparable to the curves of ZF in perfectly-known channels. Notably, a higher $f_d T$ we have, leads to BER values closer to the ZF in perfectly-known channel in fewer iterations. For example, consider $f_d T = 0.075$ and 0.1 in Fig. 5, in which the proposed method outperformed the ZF in a perfectly-known channel, because two or three iterations were sufficient to mitigate the interference induced from the pilots. This analysis shows that the 2nd iteration performance was better than the ZF in perfectly-known channels for E_b/N_0 between 15 and 32 dB. For $f_d T = 0.1$ at $\text{BER} = 1.5 \times 10^{-3}$ and $E_b/N_0 = 40$ dB, the proposed method had performance equal to ZF in a perfectly-known channel in three iterations. For $f_d T = 0.075$ at $\text{BER} = 7 \times 10^{-4}$ and $E_b/N_0 = 40$ dB, the performance gain of three iterations of our method compared to ZF in perfectly-known channel was approximately 2 dB. Furthermore, as seen in Fig. 4, the interference is not so severe for $f_d T = 0.025$ and 0.05 where the iterative results demonstrate performance close to that of ZF in perfectly-known channels. For example, with $f_d T = 0.05$ at $\text{BER} = 5 \times 10^{-4}$ and $E_b/N_0 = 40$ dB, the proposed method has a performance gain after three iterations of approximately 3.5 dB compared to ZF in perfectly-known channel. For $f_d T = 0.025$ at $\text{BER} = 1.3 \times 10^{-4}$ and $E_b/N_0 = 40$ dB, the performance gain of our method compared to ZF in perfectly-known channels after three iterations was approximately 6 dB.

In summary, the simulation results confirm that the proposed method has significantly better overall performance than the conventional method with similar computational complexity.

6 Conclusions

Under the condition of high speed movement, ICI caused by fast time-varying multipath fading channels raised by the Doppler spread significantly degrades the OFDM system performance. This study proposes a hybrid method for iterative joint channel estimation and signal detection for OFDM systems in rapidly time-varying multipath fading channels, to enhance performance in highly mobile wireless environments, assuming that the channel varies in a linear fashion in an OFDM symbol period. Simulation results and numerical analysis of the proposed method shows that it has similar in computational complexity to the traditional method while achieving superior performance. Simulation results demonstrates that the proposed method provides highly accurate channel estimation under a wide range of normalized Doppler frequencies, even under a normalized Doppler frequency as large as 0.075 and 0.1.

Acknowledgements The author would like to thank the Ministry of Science and Technology of the Republic of China, Taiwan, for financially supporting the research under Contract No. MOST 103-2218-E-539-001.

References

1. Jan, Y. H. (2015). Efficient window-based channel estimation for OFDM system in multi-path fast time-varying channels. *IEICE Transactions on Communications*, E98-B(11), 2330–2340.

2. Schniter, P. (2004). Low-complexity equalization of OFDM in doubly selective channels. *IEEE Transactions on Signal Processing*, 52(4), 1002–1011.
3. Li, Y., & Cimini, L. J. (2001). Bounds on the interchannel interference of OFDM in time varying impairments. *IEEE Transactions on Communications*, 49(3), 401–404.
4. Zemen, T., & Mecklenbrauker, C. F. (2005). Time-variant channel estimation using discrete prolate spheroidal sequences. *IEEE Transactions on Signal Processing*, 53(9), 3597–3607.
5. Zhang, J., Mu, X., Chen, E. E., & Yang, S. (2008). Decision-directed channel estimation based on iterative linear minimum mean square error for orthogonal frequency division multiplexing systems. *IET Communications*, 3(7), 1136–1143.
6. Gorokhov, A., & Linnartz, J. P. (2005). Iterative interference cancellation and channel estimation for mobile OFDM. *IEEE Transactions on Wireless Communications*, 4(1), 238–245.
7. Hijazi, H., & Ros, L. (2009). Polynomial estimation of time-varying multipath gains with ICI mitigation in OFDM systems. *IEEE Transactions on Vehicular Technology*, 58(1), 140–151.
8. Mostofi, Y., & Cox, D. (2005). ICI mitigation for pilot-aided OFDM mobile system. *IEEE Transactions on Wireless Communications*, 4(2), 765–774.
9. Kwak, K., Lee, S., Min, H., Choi, S., Lee, S., Min, H., et al. (2010). New OFDM channel estimation with dual-ICI cancellation in highly mobile channel. *IEEE Transactions on Wireless Communications*, 9(10), 3155–3165.
10. Jan, Y. H. (2015). Transmission efficient channel estimation for OFDM System under multi-path fast fading channel. *Wireless Personal Communications*, 84(2), 1561–1575.
11. Jan, Y. H. (2015). Reduced-overhead channel estimation for OFDM systems in multipath fast time-varying channels. *Journal of Internet Technology*, 16(6), 1099–1108.
12. COST 207 Management Committee. (1989) COST 207: Digital land mobile radio communications. Commission of the European Communication.



Yih-Haw Jan received the B.S. and the M.S. degrees in Electronical Engineering from Chung Hua University, Hsinchu, Taiwan, R.O.C., in 1994 and 1996, respectively. He received the Ph.D. degree in electronics engineering from National Chaio Tung University, Taiwan, R. O.C., in 2005. He was with Chuanyao Computer Corp., Taichung, during 1996–2000. He is Associate Professor of Department of Digital Living Innovation, adjunct Associate Professor with Gerontic Technology and Service Management, as well as adjunct Associate Professor of Mechanical Engineering, Nan Kai University of Technology, Taiwan, R.O.C. Since 2009, he is also an Adjunct Associate Professor of Army Academy, Taiwan, R.O.C. He has conducted research in digital subscriber line and coaxial cable network transmission, video coding, and wireless communication. His current research interests include signal processing for wireless communication.